

1 **Small-scale convection in the Earth's mantle**

2 **Maxim D. Ballmer**

3 Institute of Geophysics, Department of Earth Sciences, ETH Zurich; Earth-Life Science Institute, Tokyo Institute of
4 Technology; maxim.ballmer@erdw.ethz.ch

5

6 **Abstract**

7 Small-scale convection (SSC) in the Earth's mantle contributes to intraplate deformation, heat flow and
8 volcanism. In this review, I give an overview over the causes and effects of SSC. SSC is a boundary layer
9 instability that is driven by a density inversion, and mostly restricted to low-viscosity layers such as the
10 asthenosphere. The density inversion that supports SSC can be related to thermal and/or chemical
11 stratification. SSC is thought to occur beneath mature oceanic basins to restrict their subsidence and
12 stabilize geothermal heat flux. The onset of SSC is preferentially triggered near lateral heterogeneity such
13 as fracture zones or other steps in lithospheric thickness. SSC may also occur beneath continents, and
14 seismic evidence for related perturbations has indeed been found. Both in continental and oceanic
15 environments, SSC can cause dynamic topography, intraplate deformation, as well as melting of mantle
16 rocks. Mantle melting can boost SSC through a positive-feedback mechanism, and most importantly,
17 feeds intraplate volcanism. While plate tectonics and related natural hazards are mostly caused by large-
18 scale whole-mantle circulation, intraplate geologic activity may be sustained by SSC in the upper mantle.

19

20 **Keywords**

21 Small-scale convection, edge-driven convection, convection, mantle, buoyant decompression melting,
22 melting, volcanism, heat flow, subsidence, seafloor flattening, uplift, plume-lithosphere interaction

23

24 **1. Introduction**

25 The transport of primordial and radiogenic heat from the deep Earth's interior to the surface is mostly
26 accomplished by mantle convection. Large-scale mantle flow drives the motion of tectonic plates and is
27 thus responsible for first-order geological activity on Earth – such as mountain building, continental
28 breakup, mid-ocean ridge and subduction-related volcanism – as well as the related natural hazards.
29 Smaller scales of mantle flow, mostly occurring in the low-viscosity upper mantle, are superimposed on

30 these large scales of whole-mantle circulation, and sustain deformation within tectonic plates. Such
31 deformation can be e.g. expressed as dynamic uplift and extension (*Göğüş and Pysklywec, 2008b*), or
32 subsidence and sedimentation (*Petersen et al., 2010*). Small-scale convection (SSC) upwellings may
33 further feed mantle melting and intraplate volcanism, thus e.g. supporting seamount and ocean-island
34 formation (*Ballmer et al., 2007; Bonatti and Harrison, 1976; Bonatti et al., 1977; King, 2007*). Moreover,
35 SSC can drive the motion of microplates within mobile belts, such as in the Mediterranean (*Faccenna et*
36 *al., 2013*), and thus control first-order geologic activity along microplate boundaries. SSC might be even
37 an important mechanism for the generation of plate boundaries, e.g. by initiating subduction zones
38 (*Solomatov, 2004*). Although several articles and book chapters have been published about SSC in the
39 mantle, and some review chapters have summarized some of the related issues (e.g., *Ballmer et al.,*
40 *2015c; Parmentier, 2007*), no comprehensive review has yet been dedicated to the topic. In this module, I
41 will discuss the causes for, and consequences of, SSC in the Earth's mantle.

42

43 **2. Physical Background**

44 Convection across a fluid layer is an efficient mode of heat transport with heat being transported along
45 with the flow of anomalously warm or cold matter. Generally, convection is driven by unstable density
46 stratification. Density inversion e.g. occurs as a consequences of heating a fluid from below and/or cooling
47 from above, such that low-density warm fluid is overlain by high-density cold fluid.

48 On all scales, convection competes with other modes of heat transport. For the Earth's interior, the most
49 relevant competing mode is conduction of heat. Thermal convection is a more efficient mode than
50 conduction if the fluid layer's Rayleigh number $Ra = \alpha \rho_0 \Delta T g d^3 / \kappa \eta$ exceeds a critical value (i.e., on the
51 order of ~ 1000) (*Bénard, 1901; Turcotte and Schubert, 1982*). In this case, even infinitesimally small
52 thermal perturbations grow exponentially to sustain the formation of convection cells. As thermal
53 expansivity α , gravity g , reference density ρ_0 , and conductivity κ are well-constrained and/or near-
54 constant across the mantle, the temperature jump across the fluid layer ΔT , the layer thickness d and the
55 viscosity of the fluid η control the Rayleigh number with $Ra \sim \Delta T d^3 / \eta$.

56 In a fluid heated from below and cooled from above, convection is usually driven by thermal boundary
57 layer instability. Thin thermal boundary layers (TBL) with steep thermal gradients are sustained, because
58 conduction is more efficient than convection for small d . Convective instability usually rises out of these
59 TBL. For viscous instability developing from a cold TBL, over which the viscosity varies by several
60 orders of magnitude, the concept of a local Ra has been shown to be useful (e.g., *Parson and McKenzie,*

61 1978), because only the negative buoyancy of the viscously deformable base of the TBL is available to
62 drive convection. This situation needs to be accounted for to in determining the relevant parameters that
63 control the Ra . For convection driven by unstable compositional stratification (Rayleigh-Taylor
64 instability; see section 3.3), the relevant compositional $Ra_{comp} = \Delta\rho_{comp}gd^3/\kappa\eta$, where $\Delta\rho_{comp}$ is the
65 compositional density contrast.

66 In a fluid that is rheologically layered (and compositionally heterogeneous), such as the Earth's mantle
67 (e.g., *Mitrovica and Forte, 2004; Zindler and Hart, 1986*), convection can simultaneously occur on
68 various scales (and be manifested as thermal plus compositional — or thermochemical — convection).
69 Large-scale convective flow organizes across the whole mantle (i.e., on scales of several thousands of
70 km), because Ra becomes super-critically large for large d (and large ΔT). Smaller scales of convection
71 (i.e., of the order of hundreds of km) can organize within low-viscosity layers close to the global TBL at
72 the top or bottom of the mantle, because Ra becomes sufficiently large for low η (and significant ΔT),
73 even for rather small d (e.g., *Korenaga and Jordan, 2003; Solomatov and Moresi, 2000*). Thus, SSC may
74 occur in the asthenosphere (*Richter and Parsons, 1975*), in low-viscosity regions near the core-mantle
75 boundary (*Cizkova et al., 2010*), or even across the whole upper mantle (*Korenaga and Jordan, 2004*).
76 SSC may also develop near regional TBLs, such as the roofs of the large low shear-wave velocity
77 provinces, where small-scale “plumelets” are thought to rise and feed hotspot volcanism (*Davaille, 1999*),
78 or at the base of subducted slabs that stagnate in the mantle transition zone (*Motoki and Ballmer, 2015*).

79 The specific layer that undergoes convective instability must include a finite ΔT to maximize the relevant
80 local Ra . So, in the case of top-down driven SSC from a cold TBL, the layer must include at least the
81 relatively soft base of the TBL, and the relevant local Ra is limited by the viscosity of this base. In case of
82 bottom-up driven SSC from a hot TBL, the local Ra is in turn restricted by the viscosity and thickness of
83 the overlying layer.

84

85 **3. Styles of SSC**

86 Due to its applicability to surface geologic processes, the occurrence of SSC in the asthenosphere has
87 been most closely studied. SSC in the asthenosphere is top-down driven by a density inversion with cool
88 sublithospheric mantle overlying the warm asthenosphere, and facilitated by intrinsically low viscosities.
89 The low viscosity of the asthenosphere is thought to be sustained by the abundance of small amounts of
90 melt (*Anderson and Sammis, 1970*), a local dominance of dislocation creep (*Karato, 1987*), reduced

91 mineral grain sizes (*Faul and Jackson, 2005*), relatively large temperatures (“plume-fed asthenosphere”)
92 (*Morgan et al., 1995*), and/or relatively high water contents (*Karato and Jung, 1998*).

93 3.1 SSC beneath the oceanic lithosphere

94 A textbook case of SSC occurs beneath oceanic plates (*Richter, 1973*). Here, the sublithospheric TBL
95 grows as the plate moves away from the mid-ocean ridge (MOR). As soon as the TBL exceeds a critical
96 thickness, the local Ra becomes sufficiently large, and sublithospheric SSC initiates (*Fleitout and Yuen,*
97 *1984; Houseman and McKenzie, 1982; Parsons and McKenzie, 1978; Zaranek and Parmentier, 2004*).
98 SSC is thought to initiate beneath oceanic lithosphere of age ~ 70 Ma, depending on regional conditions.
99 Beneath significantly younger oceanic lithosphere, the TBL is thinner than the lithospheric harzburgite
100 layer, the stiff depleted residue from MOR melting (Ra is small due to high η), and hence SSC should
101 normally not occur. Beneath oceanic lithosphere of age ~ 70 Ma and older, the TBL instead extends
102 through this stiff depleted residue and into the weak asthenosphere to drive SSC (*Afonso et al., 2008;*
103 *Ballmer et al., 2009; Lee et al., 2005*).

104 SSC acts to remove the base of the TBL and replace it by warm mantle from below, thereby transporting
105 heat to the base of the lithosphere and balancing the thickness of the plate. Thus, the occurrence of SSC
106 can account for the observed flattening of seafloor topography and of heat flow on oceanic plates older
107 than ~ 70 Ma (*Cazenave et al., 1988; Crosby et al., 2006; Doin and Fleitout, 1996; Hasterok and*
108 *Chapman, 2011; Parsons and Sclater, 1977; Stein and Stein, 1994a; b*), as well as seismic estimates for
109 the thickness of the oceanic lithosphere (*Priestley and McKenzie, 2006; Ritzwoller et al., 2004*). These are
110 the main observations that support the SSC model. An alternative mechanism to account for these
111 observations involves the collective effect of the mantle plumes (*Crough, 1975; Hayes, 1988; Morgan et*
112 *al., 1995*).

113 Direct observations of SSC beneath oceanic plates instead remain controversial. SSC is predicted to
114 organize as convection rolls that are mostly confined to the low-viscosity asthenosphere (e.g., *Hall and*
115 *Parmentier, 2003; van Hunen et al., 2005*) (Fig. 1). To minimize the interaction with asthenospheric
116 shearing and large-scale flow, SSC rolls more-or-less strictly align with the direction of the overriding
117 plate (*Richter and Parsons, 1975*), depending on plate velocity and the time since the last plate
118 reorganization (*Marquart, 2001; van Hunen and Zhong, 2006*). Accordingly, SSC are predicted to be
119 associated with lineations in heat flow, gravity, seismic anomalies and seafloor topography (*Buck and*
120 *Parmentier, 1986*) with wavelengths similar to the vertical extent of the asthenosphere (but cf. *Lev and*
121 *Hager, 2008*). However, heat flow measurements and seismic tomography remain challenging in oceanic
122 basins. Also, dynamic topography associated with SSC on thick and old lithosphere is predicted to be too

123 small to be resolved (*Sleep*, 2011). On the much younger oceanic lithosphere close to the East Pacific
124 Rise, lineations in geophysical observables of wavelengths ~ 100 km have been detected, and in many
125 aspects are consistent with the effects SSC (*Harmon et al.*, 2011; *Haxby and Weissel*, 1986). Because of
126 their geographic patterns that extend to very close of the East Pacific Rise, however, these lineations are
127 difficult to be reconciled at least with the textbook case of SSC, unless the asthenospheric viscosity is
128 very low ($\sim 10^{18}$ Pa·s or smaller), and (interaction with) alternative mechanisms such as viscous fingering
129 (*Ballmer et al.*, 2013; *Weeraratne et al.*, 2007), or off-axis melting instabilities (*Barnouin-Jha et al.*,
130 1997), need to be considered. The much more extensive lineations of wavelengths 1500~2000 that are
131 evident in full-waveform S-wave tomography (*French et al.*, 2013) as well as the gravity field (*Hayn et*
132 *al.*, 2012) are also not fully consistent with sublithospheric SSC (i.e., mostly confined to the
133 asthenosphere), both because of their large wavelengths as well as their manifestation beneath young
134 oceanic plates, even crossing MORs (also see discussion). Future studies are indeed required to
135 understand the interaction of SSC with other geodynamic mechanisms (e.g., viscous fingering), as well as
136 the much larger scales of whole-mantle circulation.

137 3.2 SSC related to mantle plume activity

138 Small-scale convection can also occur in regionally restricted settings, such as in mantle plumes that pond
139 beneath the lithosphere as a “pancake” of hot material. In this specific case, the conditions mentioned
140 above in terms of the age of the lithosphere required for SSC are relaxed, because the viscosity of
141 pancake is sufficiently low (*Agrusta et al.*, 2013; *Moore et al.*, 1998; *Moore et al.*, 1999; *Thoraval et al.*,
142 2006). The manifestation of SSC in the Hawaiian plume pancake can explain the occurrence of
143 rejuvenated-stage volcanism and off-axis volcanism, the decrease geoid-to-topography ratio of the swell
144 to the WNW, as well as geochemical asymmetry of shield-building volcanism (*Ballmer et al.*, 2011;
145 *Cadio et al.*, 2012; *Garcia et al.*, 2010). In turn, SSC far away from mantle plumes (section 3.1) can
146 sustain “hot-line” volcanic chains that — in contrast to plume-fed hotspot volcanism — display coeval
147 activity over >1000 km (*Bonatti and Harrison*, 1976; *Bonatti et al.*, 1977; *Ballmer et al.*, 2007; 2009) (Fig.
148 1).

149 3.3 Compositional SSC

150 While the textbook case of SSC is exclusively driven by an inversion of thermal density, convective
151 instability may be alternatively fueled by an inversion of compositional density (i.e., Rayleigh-Taylor
152 instability (*Rayleigh*, 1913)) with high-density fluid underlain by low-density fluid. Such a situation can
153 e.g. occur near subduction zones, where the slab carries a layer of low-density materials such as
154 sediments or serpentinized basalt into the mantle. Dehydration of serpentine leads to hydration and/or

155 partial melting of overlying mantle rock. The resulting mélange of low-density rocks becomes
156 convectively unstable as soon as it is juxtaposed to the high-density peridotitic mantle wedge above
157 (*Gerya and Yuen, 2003*). In this case, a strongly unstable compositional density inversion can even
158 overcome stable thermal layering (i.e., the hot mantle wedge overlying the cool slab). Similarly,
159 compositional instability can rise out of the buoyant harzburgitic underbelly of a subducted slab that
160 stagnates in the transition zone (*Motoki and Ballmer, 2015*) or near the core-mantle boundary (*Tackley,*
161 2011).

162 Another form of compositional SSC is buoyant decompression melting (BDM) instability. A layer of rock
163 that is very close to or at its solidus may undergo localized melting due to small lateral thermal variations
164 and/or passive upwelling. Any such localized melting induces focused upwelling, because melt (as well as
165 the residue of melting) is less dense than rock. Since this upwelling in turn causes further decompression
166 melting in a positive-feedback loop, short-lived small-scale convection cells emerge (*Tackley and*
167 *Stevenson, 1993*). BDM usually ceases after one full overturn, because it runs out of fuel; the depleted
168 residue of magmatism cannot continue melting without additional heat input (*Raddick et al., 2002*) (Fig.
169 2). Nevertheless, the process of BDM can assist other mechanisms such as SSC in sustaining magmatism
170 (*Ballmer et al., 2009*). Episodes of BDM can also occur near a MOR, as initial melts are produced on-axis
171 and subsequently undergo instability off-axis (*Barnouin-Jha et al., 1997; Sparks et al., 1993*). In this case,
172 BDM is boosted by a cessation of extension and divergence as the partially molten material moves away
173 from the ridge axis (*Herlund et al., 2008a*). A cessation of extension can also trigger BMO within the
174 partially molten asthenosphere in intraplate settings (*Herlund et al., 2008b*).

175 **3.4 Edge-driven convection**

176 Convective instability is generally assisted by lateral heterogeneity. The presence of lateral heterogeneity,
177 such as fracture zones or cratonic margins, strongly reduces the timescales for the onset of convective
178 instability, and thereby acts to trigger SSC (*Dumoulin et al., 2005; Huang et al., 2003*). Thus, the most
179 vigorous and stable downwellings of SSC occur near steps of lithospheric thickness, such as the edges of
180 cratonic keels or orogenic roots (Fig. 3). Upwelling return flow is in turn focused at a distance of several
181 hundreds of km away from the step to induce uplift and magmatism (*Kaislaniemi and van Hunen, 2014;*
182 *King, 2007; Missenard and Cadoux, 2012; Shahnas and Pysklywec, 2004; Till et al., 2010; van Wijk et*
183 *al., 2010*). This variant of SSC has been dubbed “edge-driven” convection (*King and Anderson, 1998*).
184 The edge-driven convection model implies that downwellings consistently emerge along cratonic margins
185 with uplift and volcanism along a belt parallel to the margin at a distance of a few 100s of km. It has been

186 used to account for intraplate volcanism as well as seismic observations mainly on the African and South
187 American plates (*King and Ritsema, 2000; King, 2007*).

188 3.5 SSC beneath continents

189 Beneath the continents, SSC is most likely caused by a combination of mechanisms. As beneath the
190 oceans, TBL instability remains an important driving mechanism for continental SSC (see section 3.1)
191 (*Houseman et al., 1981*), but variations in composition (section 3.3) (*Houseman and Molnar, 1997; Neil
192 and Houseman, 1999*) as well as steps in lithospheric thickness (section 3.4) (*King and Anderson, 1998*)
193 are common ingredients beneath continents that can trigger SSC. Sublithospheric topography is common
194 beneath continents, and likely controls the geometry of SSC beneath the slow-moving continental plates
195 (*Fourel et al., 2013; Milelli et al., 2012*). For example, a combination of horizontal flow, edge-driven
196 convection and viscosity heterogeneity in the asthenosphere can give rise to vertical flow and magmatism
197 (*Ballmer et al., 2015a; Conrad et al., 2010; Kaislaniemi and van Hunen, 2014; Till et al., 2010*) (Fig. 3).
198 Entrainment of warm plume material or enriched slab-derived material into such upwellings may provide
199 the conditions for mantle melting (e.g., *Duggen et al., 2009*). Intraplate extension acts to advance small-
200 scale convective instability due to the induction of mantle upwelling as well as the creation of
201 sublithospheric topography (e.g., along rifts) (*Boutelier and Keen, 1999; Buck, 1986; van Wijk et al.,
202 2008; van Wijk et al., 2010*). Alternatively, underplating of dense plutonic rocks may drive top-down
203 instability (*Zhai et al., 2007*). Any related SSC has been suggested to be sufficient to even destroy stable
204 cratonic roots (e.g., *Gao et al., 2009*). In turn, compositional variations may also stabilize cratonic roots,
205 e.g. by muting SSC as a consequence of decreased lithospheric viscosity and/or density. As the viscosity
206 structure in continental plates is usually layered, deformation during convective instability may be
207 focused along weak horizons and therefore lead to the “delamination” of elongated chunks of the lower
208 crust (*Göğüş and Pysklywec, 2008b; Kay and Kay, 1993*). Accordingly, delamination of the lower crust
209 may be regarded as a variant of SSC in the presence of complex rheology (*Burov and Molnar, 2008*), in
210 which the local Ra is controlled by the viscosity of the weak zone, and strongly anisotropic viscosity
211 controls the geometry of downwellings. Delamination and dripping are two geometrical end-members of
212 SSC beneath continents.

213 Subcontinental SSC has various geological and geophysical implications. Intraplate uplift and subsidence
214 is commonly related to SSC up- and downwellings. Hence, SSC controls erosional patterns as well as
215 sustains the formation of sedimentary basins (*Petersen et al., 2010*). For example, delamination may
216 induce rapid uplift and erosion just after detachment of the lower crust, followed by persistent subsidence
217 due to focusing of downwelling flow (*Göğüş and Pysklywec, 2008a*). Beneath continents with dense

218 seismic networks, it is possible to detect isotropic and anisotropic seismic velocity anomalies that can be
219 directly related to SSC (*Alsina and Snieder, 1995; Makeyeva et al., 1992; Schmandt and Humphreys,*
220 *2010; West et al., 2009; Yang and Forsyth, 2006*). Intraplate seismicity, deformation, mountain building
221 and volcanism have also been related to SSC. While large-scale convection drives the motion of tectonic
222 plates and major geologic activity along plate boundaries, SSC can account for a wide range of intraplate
223 geological processes.

224

225 **4. Discussion**

226 A key issue regarding the “theory” of SSC in the mantle is the observability of the process. From a fluid
227 dynamics point of view, SSC is well-established and almost an inevitable product of convection in a high-
228 *Ra* fluid with significant rheological layering, as is the Earth’s mantle. Even though any methods for
229 determining the radial viscosity structure of the Earth suffer fundamental trade-offs, at least a relatively
230 weak asthenosphere and viscosity jump somewhere near 660~1,000 km depth are robust features of
231 glacial-rebound and geoid inversions, respectively (e.g., *Rudolph et al., 2015*). Also, the predictions of the
232 theory of SSC on a broader scale (e.g., seafloor flattening) are well consistent with observations, and a
233 wide range of circumstantial evidence supports the theory (see above). However, from a phenomenon
234 point of view, there are few direct observations of SSC in the mantle, and the patterns of convection
235 remain poorly constrained.

236 In recent years, at least “mid-scale” convective patterns become well in reach of proper characterization
237 by geophysical observations. Here, I consider mid-scale convection as SSC with wavelengths on the order
238 of ~1,200 to 2,000 km. For simple rheology, such mid-scale wavelengths are expected for convection
239 across the entire upper mantle, or even down to ~1,000 km depth. Such mid-scale convection is expected
240 to be sustained by progressive cooling of the asthenosphere by sublithospheric SSC, which accordingly
241 tends to break down into larger convection cells down to the base of the transition zone (*Korenaga and*
242 *Jordan, 2004*). Mid-scale convection may further rise from a second-order TBL at the base of the
243 transition zone (*Motoki and Ballmer, 2015*), for example due to limited material exchange between the
244 upper and lower mantles (*Ballmer et al., 2015b; Ballmer et al., 2017; Tackley et al., 1993*), which is also
245 evident by slab stagnation at various depths in the mid mantle (*Fukao and Obayashi, 2013; Goes et al.,*
246 *2017*). Alternatively, SSC on wavelength of 1,000-2,000 may be mostly confined to the asthenosphere if
247 the rheology, for example due to lattice-preferred orientation beneath the moving plates, is significantly
248 anisotropic (*Lev and Hager, 2008*).

249 The specific patterns of mid-scale convection (whether confined to the asthenosphere or throughout the
250 upper mantle) may be related to geophysical observations. Viable candidates are low-viscosity fingers as
251 retrieved from seismic tomography (*French et al.*, 2013; *Katzman et al.*, 1998), as well as undulations of
252 the residual (dynamic) topography (*Hoggard et al.*, 2016) and gravity field (Hayn et al., 2012) on the
253 relevant scales. It may further be mirrored by the patterns of slab sinking (and related return flow
254 (*Faccenna et al.*, 2013)) near subduction zones, and by that of microplates in mobile belts such as the
255 Mediterranean (*Faccenna et al.*, 2010). Along these lines, we may already be able to map the patterns of
256 mid-scale convection over vast regions of our planet, although continental regions without sufficient
257 seismic instrumentation remain problematic (due to lithological heterogeneity and tectonic complexity).
258 First attempts to map vertical upper-mantle flow in geophysically well-characterized continental regions
259 such as the western US are indeed promising (*Afonso et al.*, 2016; *Schmandt et al.*, 2014).

260

261 **5. Conclusion and Outlook**

262 Convection is an efficient mechanism for the transport of heat across the mantle. It is generally driven by
263 a density inversion due to the combined effects of temperature and composition. In addition to large-scale
264 convection on the order of thousands of km, small-scale convection (SSC) is thought to occur near
265 thermal and compositional boundary layers, particularly across regions of reduced mantle viscosity, such
266 as the asthenosphere. SSC should be advanced by the presence of lateral heterogeneity, for example by
267 steps of lithospheric thickness along cratonic margins or fracture zones. Beneath continents with their
268 complex geologic structures, SSC is influenced by various factors, including sublithospheric topography,
269 horizontal flow, compositional heterogeneity as well as the related effects on density and viscosity
270 structure. While only indirect evidence for the occurrence of SSC beneath mature oceanic basins is
271 provided by the flattening of seafloor topography (and heat flow), direct evidence for the occurrence of
272 SSC beneath continents comes from seismic observations.

273 Future work is required to better understand the interplay between large-scale and small-scale flow in the
274 global context. Large-scale whole-mantle convection should influence the patterns of SSC by driving
275 shear flow in the asthenosphere, and by sustaining large-scale thermal perturbations that will delay or
276 advance SSC through their effects on viscosity. Also, large-scale flow may set up boundary layers in the
277 mid-mantle or transition zone, from which SSC instability may develop, for example near stagnant slabs
278 (*Fukao and Obayashi*, 2013) or ponding/deflected plumes (*French and Romanowicz*, 2015; *Kumagai et*
279 *al.*, 2008). Furthermore, the effects of mineral grain-size and fabric on mantle rheology and SSC, and

280 vice-versa, require detailed further study. Perhaps most importantly, future efforts should be focused on
281 detecting the signals and patterns of SSC. For example, direct seismic evidence for the occurrence of
282 sublithospheric SSC beneath the oceans on the expected wavelength of several 100s of km remains
283 elusive. Systematic comparison of model predictions and observations will lead to great insight into the
284 underlying mantle dynamics and dominant rheological mechanisms.

285

286 **6. References**

- 287 Afonso, C. A., S. Zlotnik, and M. Fernandez (2008), Effects of compositional and rheological
288 stratifications on small-scale convection under the oceans: Implications for the thickness of
289 oceanic lithosphere and seafloor flattening, *Geophys. Res. Lett.*, *35*, doi:L20308.
- 290 Afonso, J. C., N. Rawlinson, Y. Yang, D. L. Schutt, A. G. Jones, J. Fullea, and W. L. Griffin (2016), 3-D
291 multiobservable probabilistic inversion for the compositional and thermal structure of the
292 lithosphere and upper mantle: III. Thermochemical tomography in the Western-Central US,
293 *Journal of Geophysical Research: Solid Earth*, *121*(10), 7337-7370.
- 294 Agrusta, R., D. Arcay, A. Tommasi, A. Davaille, N. Ribe, and T. Gerya (2013), Small-scale convection in
295 a plume-fed low-viscosity layer beneath a moving plate, *Geophys. J. Int.*, ggt128.
- 296 Alsina, D., and R. Snieder (1995), Small-scale sublithospheric continental mantle deformation:
297 constraints from SKS splitting observations, *Geophys. J. Int.*, *123*(2), 431-448.
- 298 Anderson, D. L., and C. Sammis (1970), Partial melting in the upper mantle, *Phys. Earth Planet. Int.*, *3*,
299 41-50.
- 300 Ballmer, M. D., J. van Hunen, G. Ito, P. J. Tackley, and T. A. Bianco (2007), Non-hotspot volcano chains
301 originating from small-scale sublithospheric convection, *Geophys. Res. Lett.*, *34*(23),
302 doi:doi:10.1029/2007GL031636.
- 303 Ballmer, M. D., J. van Hunen, G. Ito, T. A. Bianco, and P. J. Tackley (2009), Intraplate volcanism with
304 complex age-distance patterns – a case for small-scale sublithospheric convection, *Geochem.*
305 *Geophys. Geosyst.*, *10*, Q06015, doi:10.1029/2009gc002386.
- 306 Ballmer, M. D., G. Ito, J. van Hunen, and P. J. Tackley (2011), Spatial and temporal variability in
307 Hawaiian hotspot volcanism induced by small-scale convection, *Nature Geoscience*, *4*(7), 457-
308 460, doi:10.1038/ngeo1187.
- 309 Ballmer, M. D., C. P. Conrad, E. I. Smith, and N. Harmon (2013), Non-hotspot volcano chains produced
310 by migration of shear-driven upwelling toward the East Pacific Rise, *Geology*, *41*(4), 479-482,
311 doi:10.1130/g33804.1.
- 312 Ballmer, M. D., C. P. Conrad, E. I. Smith, and R. Johnsen (2015a), Intraplate volcanism at the edges of
313 the Colorado Plateau sustained by a combination of triggered edge-driven convection and shear-
314 driven upwelling, *Geochemistry, Geophysics, Geosystems*, *16*(2), 366-379,
315 doi:10.1002/2014GC005641.
- 316 Ballmer, M. D., N. C. Schmerr, T. Nakagawa, and J. Ritsema (2015b), Compositional mantle layering
317 revealed by slab stagnation at ~1000-km depth, *Science Advances*, *1*(11),
318 doi:10.1126/sciadv.1500815.
- 319 Ballmer, M. D., P. E. van Keken, and G. Ito (2015c), 7.10 - Hotspots, Large Igneous Provinces, and
320 Melting Anomalies, in *Treatise on Geophysics (Second Edition)*, edited by G. Schubert, pp. 393-
321 459, Elsevier, Oxford.
- 322 Ballmer, M. D., C. Houser, J. W. Hernlund, R. M. Wentzcovitch, and K. Hirose (2017), Persistence of
323 strong silica-enriched domains in the Earth's lower mantle, *Nature Geoscience*, *10*(3), 236-240,
324 doi:10.1038/ngeo2898.

325 Barnouin-Jha, K., E. M. Parmentier, and D. W. Sparks (1997), Buoyant mantle upwelling and crustal
326 production at oceanic spreading centers: On-axis segmentation and off-axis melting, *J. Geophys.*
327 *Res.*, *102*, 11979-11990.

328 Bénard, H. (1901), The cellular whirlpools in a liquid sheet transporting heat by convection in a
329 permanent regime, *Annales De Chimie Et De Physique*, *23*, 62-101.

330 Bianco, T. A., C. P. Conrad, and E. I. Smith (2011), Time dependence of intraplate volcanism caused by
331 shear-driven upwelling of low-viscosity regions within the asthenosphere, *J. Geophys. Res.*, *116*,
332 doi:10.1029/2011jb008270.

333 Bonatti, E., and C. G. A. Harrison (1976), Hot Lines in the Earths Mantle, *Nature*, *263*(5576), 402-404.

334 Bonatti, E., C. G. A. Harrison, D. E. Fisher, J. Honnorez, J. G. Schilling, J. J. Stipp, and M. Zentilli
335 (1977), Easter Volcanic Chain (Southeast Pacific) - Mantle Hot Line, *J. Geophys. Res.*, *82*(17),
336 2457-2478.

337 Boutilier, R., and C. Keen (1999), Small-scale convection and divergent plate boundaries, *Journal of*
338 *Geophysical Research: Solid Earth*, *104*(B4), 7389-7403.

339 Buck, W. R. (1986), Small-scale convection induced by passive rifting: the cause for uplift of rift
340 shoulders, *Earth Planet. Sci. Lett.*, *77*(3-4), 362-372.

341 Buck, W. R., and E. M. Parmentier (1986), Convection beneath young oceanic lithosphere: Implications
342 for thermal structure and gravity, *J. Geophys. Res.*, *91*(B2), 1961-1974.

343 Burov, E., and P. Molnar (2008), Small and large-amplitude gravitational instability of an elastically
344 compressible viscoelastic Maxwell solid overlying an inviscid incompressible fluid: dependence
345 of growth rates on wave number and elastic constants at low Deborah numbers, *Earth Planet. Sci.*
346 *Lett.*, *275*(3), 370-381.

347 Cadio, C., M. D. Ballmer, I. Panet, M. Diament, and N. Ribe (2012), New constraints on the origin of the
348 Hawaiian swell from wavelet analysis of the geoid to topography ratio, *Earth Planet. Sci. Lett.*,
349 *359-360*(0), 40-54, doi:10.1016/j.epsl.2012.10.006.

350 Cazenave, A., K. Dominh, M. Rabinowicz, and G. Ceuleneer (1988), Geoid and Depth Anomalies Over
351 Ocean Swells and Troughs - Evidence Of an Increasing Trend Of the Geoid to Depth Ratio With
352 Age Of Plate, *Journal Of Geophysical Research Solid Earth and Planets*, *93*(B7), 8064-8077.

353 Cizkova, H., O. Cadek, C. Matyska, and D. A. Yuen (2010), Implications of post-perovskite transport
354 properties for core-mantle dynamics, *Phys. Earth Planet. Inter.*, *180*(3-4), 235-243,
355 doi:10.1016/j.pepi.2009.08.008.

356 Conrad, C. P., B. Wu, E. I. Smith, T. A. Bianco, and A. Tibbetts (2010), Shear-driven upwelling induced
357 by lateral viscosity variations and asthenospheric shear: A mechanism for intraplate volcanism,
358 *Phys. Earth Planet. Inter.*, *178*(3-4), 162-175, doi:10.1016/j.pepi.2009.10.001.

359 Crosby, A. G., D. McKenzie, and J. G. Sclater (2006), The relationship between depth, age and gravity in
360 the oceans, *Geophys. J. Int.*, *166*(2), 553-573, doi:10.1111/j.1365-246X.2006.03015.x.

361 Crough, S. T. (1975), Thermal model of oceanic lithosphere, *Nature*, *256*(5516), 388-390.

362 Davaille, A. (1999), Simultaneous generation of hotspots and superswells by convection in a
363 heterogeneous planetary mantle, *Nature*, *402*(6763), 756-760.

364 Doin, M. P., and L. Fleitout (1996), Thermal Evolution Of the Oceanic Lithosphere - an Alternative
365 View, *Earth Planet. Sci. Lett.*, *142*(1-2), 121-136.

366 Duggen, S., K. Hoernle, F. Hauff, A. Kluegel, M. Bouabdellah, and M. Thirlwall (2009), Flow of Canary
367 mantle plume material through a subcontinental lithospheric corridor beneath Africa to the
368 Mediterranean, *Geology*, *37*(3), 283-286.

369 Dumoulin, C., M. P. Doin, D. Arcay, and L. Fleitout (2005), Onset of small-scale instabilities at the base
370 of the lithosphere: scaling laws and role of pre-existing lithospheric structures, *Geophys. J. Int.*,
371 *160*(1), 344-356.

372 Faccenna, C., T. W. Becker, S. Lallemand, Y. Lagabrielle, F. Funiciello, and C. Piromallo (2010),
373 Subduction-triggered magmatic pulses: A new class of plumes?, *Earth Planet. Sci. Lett.*, *299*(1-
374 2), 54-68, doi:10.1016/j.epsl.2010.08.012.

375 Faccenna, C., T. W. Becker, C. P. Conrad, and L. Husson (2013), Mountain building and mantle
376 dynamics, *Tectonics*, 32(1), 80-93.

377 Faul, U. H., and I. Jackson (2005), The seismological signature of temperature and grain size variations in
378 the upper mantle *Earth Planet. Sci. Lett.*, 234(1-2), 119-134.

379 Fleitout, L., and D. A. Yuen (1984), Secondary Convection and the Growth Of the Oceanic Lithosphere,
380 *Phys. Earth Planet. Inter.*, 36(SI), 181-212.

381 Fourel, L., L. Milelli, C. Jaupart, and A. Limare (2013), Generation of continental rifts, basins, and swells
382 by lithosphere instabilities, *Journal of Geophysical Research: Solid Earth*, 118(6), 3080-3100.

383 French, S., V. Lekic, and B. Romanowicz (2013), Waveform Tomography Reveals Channeled Flow at the
384 Base of the Oceanic Asthenosphere, *Science*, 342(6155), 227-230, doi:10.1126/science.1241514.

385 French, S. W., and B. Romanowicz (2015), Broad plumes rooted at the base of the Earth's mantle beneath
386 major hotspots, *Nature*, 525(7567), 95+, doi:10.1038/nature14876.

387 Fukao, Y., and M. Obayashi (2013), Subducted slabs stagnant above, penetrating through, and trapped
388 below the 660 km discontinuity, *Journal of Geophysical Research-Solid Earth*, 118(11), 5920-
389 5938, doi:10.1002/2013jb010466.

390 Gao, S., J. Zhang, W. Xu, and Y. Liu (2009), Delamination and destruction of the North China Craton,
391 *Chinese Science Bulletin*, 54(19), 3367.

392 Garcia, M. O., L. Swinnard, D. Weis, A. R. Greene, T. Tagami, H. Sano, and C. E. Gandy (2010),
393 Petrology, Geochemistry and Geochronology of Kaua'i Lavas over 4 center dot 5 Myr:
394 Implications for the Origin of Rejuvenated Volcanism and the Evolution of the Hawaiian Plume,
395 *J. Petrol.*, 51(7), 1507-1540, doi:10.1093/petrology/egq027.

396 Gerya, T. V., and D. A. Yuen (2003), Rayleigh-Taylor instabilities from hydration and melting propel
397 'cold plumes' at subduction zones, *Earth & Planetary Science Letters*, 212(1-2), 47-62.

398 Goes, S., R. Agrusta, J. van Hunen, and F. Garel (2017), Subduction-transition zone interaction: A
399 review, *Geosphere*, 13(3), 644-664, doi:10.1130/ges01476.1.

400 Göğüş, O. H., and R. N. Pysklywec (2008a), Mantle lithosphere delamination driving plateau uplift and
401 synconvergent extension in eastern Anatolia, *Geology*, 36(9), 723-726.

402 Göğüş, O. H., and R. N. Pysklywec (2008b), Near-surface diagnostics of dripping or delaminating
403 lithosphere, *Journal of Geophysical Research-Solid Earth*, 113, B11404,
404 doi:10.1029/2007jb005123.

405 Hall, C. E., and E. M. Parmentier (2003), Influence of grain size evolution on convective instability,
406 *Geochemistry Geophysics Geosystems*, 4, doi:10.1029/2002gc000308.

407 Harmon, N., D. W. Forsyth, D. S. Weeraratne, Y. Yang, and S. C. Webb (2011), Mantle heterogeneity
408 and off axis volcanism on young Pacific lithosphere, *Earth Plan. Sci. Lett.*, 311(3-4), 306-315,
409 doi:10.1016/j.epsl.2011.09.038.

410 Hasterok, D., and D. Chapman (2011), Heat production and geotherms for the continental lithosphere,
411 *Earth Planet. Sci. Lett.*, 307(1), 59-70.

412 Haxby, W. F., and J. K. Weissel (1986), Evidence For Small-Scale Mantle Convection From Seasat
413 Altimeter Data, *J. Geophys. Res.*, 91(B3), 3507-Continues.

414 Hayes, D. E. (1988), Age-depth relationship and depth anomalies in the Southeast Indian and South
415 Atlantic Ocean, *Journal of Geophysical Research-Solid Earth and Planets*, 93(B4), 2937-2954.

416 Hayn, M., I. Panet, M. Diament, M. Holschneider, M. Manda, and A. Davaille (2012), Wavelet-based
417 directional analysis of the gravity field: evidence for large-scale undulations, *Geophys. J. Int.*,
418 189(3), 1430-1456, doi:10.1111/j.1365-246X.2012.05455.x.

419 Hernlund, J. W., D. J. Stevenson, and P. J. Tackley (2008a), Buoyant melting instabilities beneath
420 extending lithosphere: 2. Linear analysis, *Journal of Geophysical Research-Solid Earth*, 113(B4),
421 doi:10.1029/2006jb004863.

422 Hernlund, J. W., P. J. Tackley, and D. J. Stevenson (2008b), Buoyant melting instabilities beneath
423 extending lithosphere: 1. Numerical models, *Journal of Geophysical Research-Solid Earth*,
424 113(B4), doi:10.1029/2006jb004862.

425 Hoggard, M., N. White, and D. Al-Attar (2016), Global dynamic topography observations reveal limited
426 influence of large-scale mantle flow, *Nature Geoscience*.

427 Houseman, G., and D. P. McKenzie (1982), Numerical Experiments On the Onset Of Convective
428 Instability In the Earths Mantle, *Geophys. J. R. Astron. Soc. (UK)*, 68(1), 133-164.

429 Houseman, G. A., D. P. McKenzie, and P. Molnar (1981), Convective instability of a thickened
430 boundary-layer and its relevance for the thermal evolution of Continental Convergent Belts, *J.*
431 *Geophys. Res.*, 86(NB7), 6115-6132, doi:10.1029/JB086iB07p06115.

432 Houseman, G. A., and P. Molnar (1997), Gravitational (Rayleigh-Taylor) instability of a layer with non-
433 linear viscosity and convective thinning of continental lithosphere, *Geophys. J. Int.*, 128(1), 125-
434 150.

435 Huang, J. S., S. J. Zhong, and J. van Hunen (2003), Controls on sublithospheric small-scale convection, *J.*
436 *Geophys. Res.*, 108(B8), 2405.

437 Kaislaniemi, L., and J. van Hunen (2014), Dynamics of lithospheric thinning and mantle melting by edge-
438 driven convection: Application to Moroccan Atlas mountains, *Geochemistry, Geophysics,*
439 *Geosystems*, 15(8), 3175-3189, doi:10.1002/2014GC005414.

440 Karato, S.-i., and H. Jung (1998), Water, partial melting and the origin of the seismic low velocity and
441 high attenuation zone in the upper mantle, *Earth Plan. Sci. Lett.*, 157(3-4), . 193-207.

442 Karato, S. (1987), Seismic anisotropy due to lattice preferred orientation of minerals: Kinematic or
443 dynamic?, in *High-Pressure Research in Mineral Physics*, edited by M. H. Manghnani and S.
444 Syono, pp. 455-471, *Geophys. Monogr. AGU*.

445 Katzman, R., L. Zhao, and T. H. Jordan (1998), High-resolution, two-dimensional vertical tomography of
446 the central Pacific mantle using ScS reverberations and frequency-dependent travel times,
447 *Journal of Geophysical Research: Solid Earth*, 103(B8), 17933-17971.

448 Kay, R. W., and S. M. Kay (1993), Delamination and Delamination Magmatism, *Tectonophysics*, 219(1-
449 3), 177-189.

450 King, S. D., and D. L. Anderson (1998), Edge-Driven Convection, *Earth & Planetary Science Letters*,
451 160(3-4), 289-296.

452 King, S. D., and J. Ritsema (2000), African hot spot volcanism: small-scale convection in the upper
453 mantle beneath cratons, *Science*, 290(5494), 1137-1140.

454 King, S. D. (2007), Hotspots and edge-driven convection, *Geology*, 35(3), 223-226,
455 doi:10.1130/g23291a.1.

456 Korenaga, J., and T. H. Jordan (2003), Linear stability analysis of Richter rolls, *Geophys. Res. Lett.*,
457 30(22), 2157.

458 Korenaga, J., and T. H. Jordan (2004), Physics of multiscale convection in Earth's mantle: Evolution of
459 sublithospheric convection, *Journal of Geophysical Research-Solid Earth*, 109(B1), 1405.

460 Kumagai, I., A. Davaille, K. Kurita, and E. Stutzmann (2008), Mantle plumes: Thin, fat, successful, or
461 failing? Constraints to explain hot spot volcanism through time and space, *Geophys. Res. Lett.*,
462 35(16), L16301, doi:10.1029/2008gl035079.

463 Lee, C. T. A., A. Lenardic, C. M. Cooper, F. L. Niu, and A. Levander (2005), The role of chemical
464 boundary layers in regulating the thickness of continental and oceanic thermal boundary layers,
465 *Earth Planet. Sci. Lett.*, 230(3-4), 379-395, doi:10.1016/j.epsl.2004.11.019.

466 Lev, E., and B. H. Hager (2008), Rayleigh-Taylor instabilities with anisotropic lithospheric viscosity,
467 *Geophys. J. Int.*, 173(3), 806-814, doi:10.1111/j.1365-246X.2008.03731.x.

468 Makeyeva, L., L. Vinnik, and S. Roecker (1992), Shear-wave splitting and small-scale convection in the
469 continental upper mantle.

470 Marquart, G. (2001), On the geometry of mantle flow beneath drifting lithospheric plates, *Geophys. J.*
471 *Int.*, 144, 356 - 372.

472 Milelli, L., L. Fourel, and C. Jaupart (2012), A lithospheric instability origin for the Cameroon Volcanic
473 Line, *Earth Planet. Sci. Lett.*, 335, 80-87.

474 Missenard, Y., and A. Cadoux (2012), Can Moroccan Atlas lithospheric thinning and volcanism be
475 induced by Edge-Driven Convection?, *Terra Nova*, 24(1), 27-33.

476 Mitrovica, J., and A. Forte (2004), A new inference of mantle viscosity based upon joint inversion of
477 convection and glacial isostatic adjustment data, *Earth Planet. Sci. Lett.*, 225(1), 177-189.

478 Moore, W. B., G. Schubert, and P. J. Tackley (1998), Three-Dimensional Simulations of Plume-
479 Lithosphere Interaction at the Hawaiian Swell, *Science*, 279, 1008-1011.

480 Moore, W. B., G. Schubert, and P. J. Tackley (1999), The role of rheology in lithospheric thinning by
481 mantle plumes, *Geophys. Res. Lett. (USA)*, 26(8), 1073-1076.

482 Morgan, J. P., W. J. Morgan, Y.-S. Zhang, and W. H. F. Smith (1995), Observational hints for a plume-
483 fed, sub-oceanic asthenosphere and its role in mantle convection, *J. Geophys. Res.*, *submitted*.

484 Motoki, M. H., and M. D. Ballmer (2015), Intraplate volcanism due to convective instability of stagnant
485 slabs in the Mantle Transition Zone, *Geochemistry, Geophysics, Geosystems*,
486 doi:10.1002/2014GC005608.

487 Neil, E. A., and G. A. Houseman (1999), Rayleigh-Taylor instability of the upper mantle and its role in
488 intraplate orogeny, *Geophys. J. Int.*, 138(1), 89-107.

489 Parmentier, E. M. (2007), 7.07 - The Dynamics and Convective Evolution of the Upper Mantle A2 -
490 Schubert, Gerald, in *Treatise on Geophysics*, edited, pp. 305-323, Elsevier, Amsterdam,
491 doi:doi:10.1016/B978-044452748-6.00121-8.

492 Parsons, B., and J. G. Sclater (1977), An analysis of the variation of ocean floor bathymetry and heat flow
493 with age, *J. Geophys. Res.*, 82(5), 803-827.

494 Parsons, B., and D. McKenzie (1978), Mantle Convection and thermal structure of plates, *J. Geophys.*
495 *Res.*, 83(NB9), 4485-4496.

496 Petersen, K. D., S. B. Nielsen, O. R. Clausen, R. Stephenson, and T. Gerya (2010), Small-Scale Mantle
497 Convection Produces Stratigraphic Sequences in Sedimentary Basins, *Science*, 329(5993), 827-
498 830, doi:10.1126/science.1190115.

499 Priestley, K., and D. McKenzie (2006), The thermal structure of the lithosphere from shear wave
500 velocities, *Earth Planet. Sci. Lett.*, 244(1-2), 285-301.

501 Raddick, M. J., E. M. Parmentier, and D. S. Scheirer (2002), Buoyant decompression melting: A possible
502 mechanism for intraplate volcanism, *J. Geophys. Res.*, 107(B10), 2228.

503 Rayleigh (1913), Motion of a viscous fluid, *Philosophical Magazine*, 26, 776-786.

504 Richter, F. M. (1973), Convection and the large-scale circulation of the mantle, *J. Geophys. Res.*, 78(35),
505 8735-8745.

506 Richter, F. M., and B. Parsons (1975), On the interaction of two scales of convection in the mantle, *J.*
507 *Geophys. Res.*, 80(17), 2529-2541.

508 Ritzwoller, M. H., N. M. Shapiro, and S. J. Zhong (2004), Cooling history of the Pacific lithosphere,
509 *Earth Planet. Sci. Lett.*, 226(1-2), 69-84, doi:10.1016/j.epsl.2004.07.032.

510 Rudolph, M. L., V. Lekić, and C. Lithgow-Bertelloni (2015), Viscosity jump in Earth's mid-mantle,
511 *Science*, 350(6266), 1349-1352, doi:10.1126/science.aad1929.

512 Schmandt, B., and E. Humphreys (2010), Complex subduction and small-scale convection revealed by
513 body-wave tomography of the western United States upper mantle, *Earth Plan. Sci. Lett.*, 297(3-
514 4), 435-445, doi:10.1016/j.epsl.2010.06.047.

515 Schmandt, B., S. D. Jacobsen, T. W. Becker, Z. Liu, and K. G. Dueker (2014), Dehydration melting at the
516 top of the lower mantle, *Science*, 344(6189), 1265-1268.

517 Shahnas, M. H., and R. N. Pysklywec (2004), Anomalous topography in the western Atlantic caused by
518 edge-driven convection, *Geophys. Res. Lett.*, 31(18).

519 Sleep, N. H. (2011), Seismically observable features of mature stagnant-lid convection at the base of the
520 lithosphere: Some scaling relationships, *Geochemistry, Geophysics, Geosystems*, 12(10), n/a-n/a,
521 doi:10.1029/2011GC003760.

522 Solomatov, V. S., and L.-N. Moresi (2000), Scaling of time-dependent stagnant lid convection:
523 Application to small-scale convection on Earth and other terrestrial planets., *J. Geophys. Res.*,
524 105(B9), 21795-21817.

525 Solomatov, V. S. (2004), Initiation of subduction by small-scale convection, *J. Geophys. Res.*,
526 109(B01412), doi:10.1029/2003JB002628.

527 Sparks, D. W., E. M. Parmentier, and J. P. Morgan (1993), 3-Dimensional Mantle Convection Beneath a
528 Segmented Spreading Center - Implications For Along-Axis Variations In Crustal Thickness and
529 Gravity, *Journal Of Geophysical Research-Solid Earth*, 98(B12), 21977-21995.

530 Stein, C. A., and S. Stein (1994a), Constraints On Hydrothermal Heat-Flux Through the Oceanic
531 Lithosphere From Global Heat-Flow, *Journal Of Geophysical Research-Solid Earth*, 99(B2),
532 3081-3095.

533 Stein, C. A., and S. Stein (1994b), Comparison Of Plate and Asthenospheric Flow Models For the
534 Thermal Evolution Of Oceanic Lithosphere, *Geophys. Res. Lett.*, 21(8), 709-712.

535 Tackley, P. J., and D. J. Stevenson (1993), A mechanism for spontaneous self-perpetuating volcanism on
536 the terrestrial planets, in *Flow and Creep in the Solar System: Observations, Modeling and*
537 *Theory*, edited by D. B. Stone and S. K. Runcorn, pp. 307-322, Kluwer.

538 Tackley, P. J., D. J. Stevenson, G. A. Glatzmaier, and G. Schubert (1993), Effects of an endothermic
539 phase transition at 670 km depth in a spherical model of convection in the Earth's mantle, *Nature*,
540 361(6414), 699-704.

541 Tackley, P. J. (2011), Living dead slabs in 3-D: The dynamics of compositionally-stratified slabs entering
542 a "slab graveyard" above the core-mantle boundary, *Phys. Earth Planet. Inter.*, 188(3), 150-162.

543 Thoraval, C., A. Tommasi, and M. P. Doin (2006), Plume-lithosphere interaction beneath a fast-moving
544 plate, *Geophys. Res. Lett.*, 33(L01301), doi:10.1029/2005GL024047.

545 Till, C. B., L. T. Elkins-Tanton, and K. M. Fischer (2010), A mechanism for low-extent melts at the
546 lithosphere-asthenosphere boundary, *Geochemistry Geophysics Geosystems*, 11,
547 10.1029/2010gc003234, doi:Q10015.

548 Turcotte, D. L., and G. Schubert (1982), *Geodynamics: Applications of Continuum Physics to Geological*
549 *Problems*, Wiley, New York.

550 van Hunen, J., S. J. Zhong, N. M. Shapiro, and M. H. Ritzwoller (2005), New evidence for dislocation
551 creep from 3-D geodynamic modeling of the Pacific upper mantle structure, *Earth Plan. Sci.*
552 *Lett.*, 238(1-2), 146-155.

553 van Hunen, J., and S. Zhong (2006), Influence of rheology on realignment of mantle convective structure
554 with plate motion after a plate reorganization, *Geochem., Geophys., Geosyst.*, 7, Q08008,
555 doi:10.1029/2005GC001209.

556 van Wijk, J., J. van Hunen, and S. Goes (2008), Small-scale convection during continental rifting:
557 Evidence from the Rio Grande rift, *Geology*, 36(7), 575-578, doi:10.1130/g24691a.1.

558 van Wijk, J. W., W. S. Baldrige, J. van Hunen, S. Goes, R. Aster, D. D. Coblenz, S. P. Grand, and J. Ni
559 (2010), Small-scale convection at the edge of the Colorado Plateau: Implications for topography,
560 magmatism, and evolution of Proterozoic lithosphere, *Geology*, 38(7), 611-614,
561 doi:10.1130/g31031.1.

562 Weeraratne, D. S., D. W. Forsyth, Y. Yang, and S. C. Webb (2007), Rayleigh wave tomography beneath
563 intraplate volcanic ridges in the South Pacific, *J. Geophys. Res.*, 112, B06303,
564 doi:06310.01029/02006JB004403.

565 West, J. D., M. J. Fouch, J. B. Roth, and L. T. Elkins-Tanton (2009), Vertical mantle flow associated with
566 a lithospheric drip beneath the Great Basin, *Nature Geoscience*, 2(6), 438-443,
567 doi:10.1038/ngeo526.

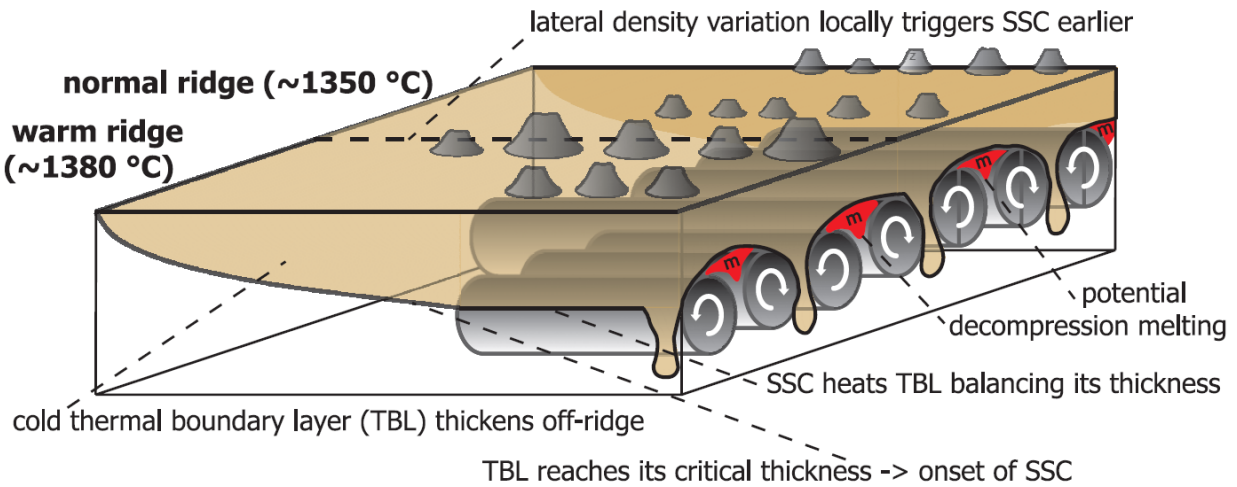
568 Yang, Y., and D. W. Forsyth (2006), Rayleigh wave phase velocities, small-scale convection, and
569 azimuthal anisotropy beneath southern California, *Journal of Geophysical Research: Solid Earth*,
570 111(B7), n/a-n/a, doi:10.1029/2005JB004180.

571 Zaranek, S. E., and E. M. Parmentier (2004), The onset of convection in fluids with strongly temperature-
572 dependent viscosity cooled from above with implications for planetary lithospheres, *Earth Planet.*
573 *Sci. Lett.*, 224(3-4), 371-386, doi:10.1016/j.epsl.2004.05.013.

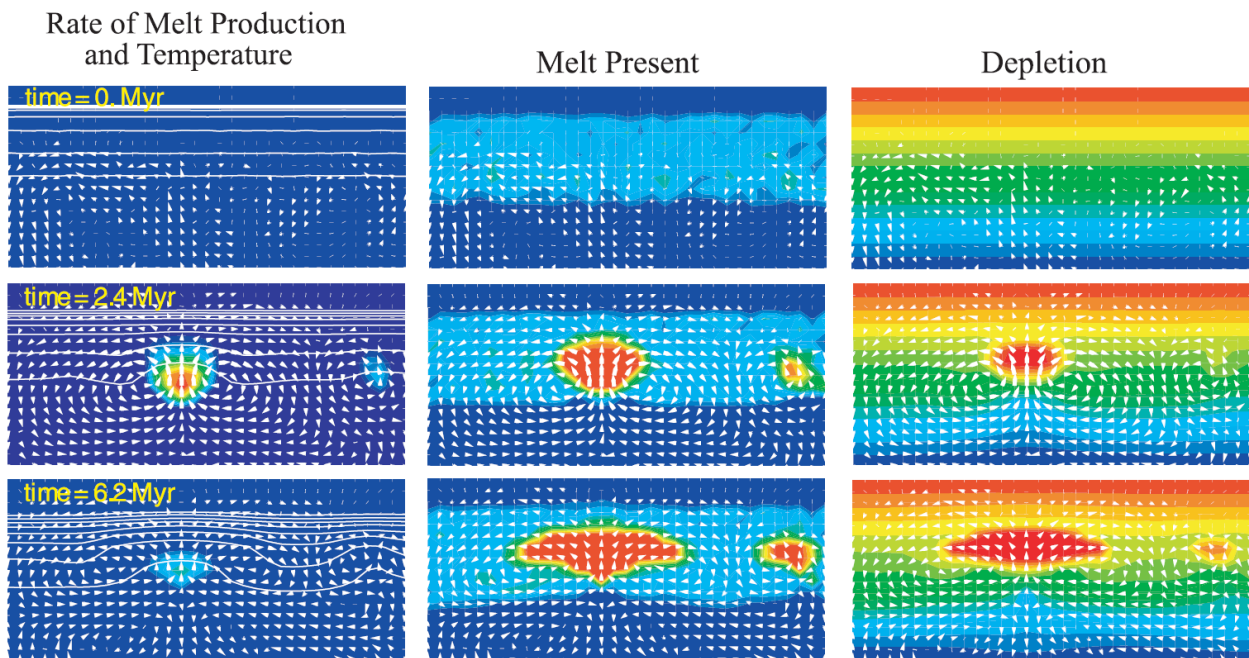
574 Zhai, M., Q. Fan, H. Zhang, J. Sui, and J. a. Shao (2007), Lower crustal processes leading to Mesozoic
575 lithospheric thinning beneath eastern North China: underplating, replacement and delamination,
576 *Lithos*, 96(1), 36-54.

577 Zindler, A., and S. Hart (1986), Geochemical geodynamics, *Earth Planet. Sci. Lett.*, 14, 493-571.

578 **7. Figures**



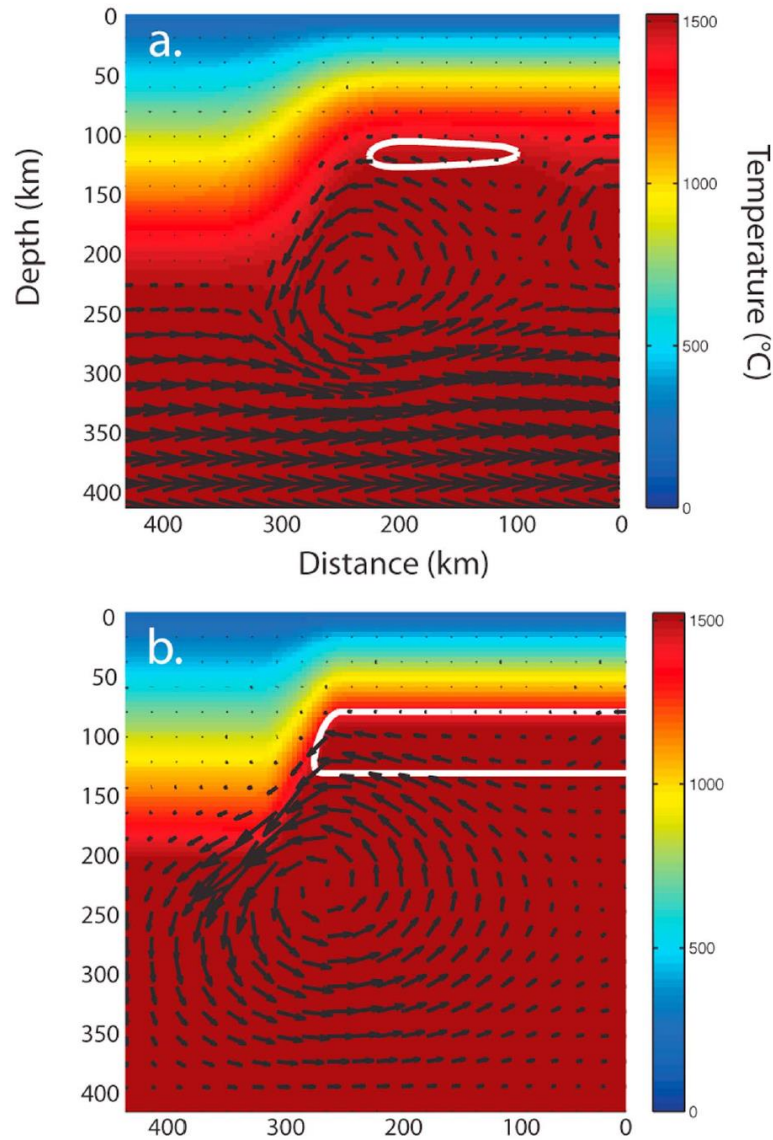
579
 580 **Fig. 1:** Cartoon of sublithospheric SSC beneath the oceanic lithosphere that grows as a function
 581 of seafloor age. At a critical seafloor age, SSC rolls develop and may potentially sustain
 582 decompression melting and coeval volcanism over large along-plate distances. Figure is
 583 reproduced from *Ballmer et al. (2009)* reprinted with the permission of the *American Geophysical*
 584 *Union.*



585
 586 **Fig. 2:** Numerical model predictions of buoyant decompression melting (BDM). Colors show
 587 melt production rate (left column), melt retention (center) and depletion (right); arrows mark
 588 direction and speed of mantle flow; lines show isotherms (left only). From top to bottom, panels

589 show snapshots as model time (as annotated) increases. BDM develops from an instability of an
590 initial melt layer (top center). It proceeds for several million years, and is shut off as depletion in
591 the convection cell progressively increases (bottom right). Figure is reproduced from *Raddick et*
592 *al.* (2002), reprinted with the permission of the *American Geophysical Union*.

593



594

595 **Fig. 3:** Edge-driven convection (EDC) with (a) and without (b) asthenospheric shear-flow in the
596 background mantle. Colors and arrows reflect mantle temperature and flow, respectively. The
597 white contour (solidus) outlines the zone of potential mantle melting. EDC alone, or an
598 interaction of EDC with “shear-driven upwelling” (*Bianco et al.*, 2011; *Conrad et al.*, 2010) due
599 to the upward deflection of horizontal flow at a step of lithospheric thickness can sustain mantle
600 melting. Figure is reproduced from *Till et al.* (2010), reprinted with the permission of the
601 *American Geophysical Union*.